

Purkinje cell dysfunction and delayed death in plasma membrane calcium ATPase 2-heterozygous mice

Amanda K. Fakira^{a,b}, Lawrence D. Gaspers^c, Andrew P. Thomas^c, Hong Li^d,
Mohit R. Jain^d, Stella Elkabes^{a,e,*}

^a Department of Neurological Surgery, University of Medicine and Dentistry of New Jersey, New Jersey Medical School, Newark, NJ, USA

^b Graduate School of Biomedical Sciences, University of Medicine and Dentistry of New Jersey, New Jersey Medical School, Newark, NJ, USA

^c Department of Pharmacology and Physiology, University of Medicine and Dentistry of New Jersey, New Jersey Medical School, Newark, NJ, USA

^d Department of Biochemistry and Molecular Biology and the Center for Advanced Proteomics Research, University of Medicine and Dentistry of New Jersey, New Jersey Medical School, Newark, NJ, USA

^e Spine Center of New Jersey, The Reynolds Family Spine Laboratory, University of Medicine and Dentistry of New Jersey, New Jersey Medical School, Newark, NJ, USA

ARTICLE INFO

Article history:

Received 14 March 2012

Revised 7 June 2012

Accepted 2 July 2012

Available online 10 July 2012

Keywords:

Ataxia
Autism
Neurodegeneration
Glutamate
AMPA
Calcium channel
Ion pump
Nitric oxide

ABSTRACT

Purkinje cell (PC) dysfunction or death has been implicated in a number of disorders including ataxia, autism and multiple sclerosis. Plasma membrane calcium ATPase 2 (PMCA2), an important calcium (Ca^{2+}) extrusion pump that interacts with synaptic signaling complexes, is most abundantly expressed in PCs compared to other neurons. Using the PMCA2 heterozygous mouse as a model, we investigated whether a reduction in PMCA2 levels affects PC function. We focused on Ca^{2+} signaling and the expression of glutamate receptors which play a key role in PC function including synaptic plasticity. We found that the amplitude of depolarization and 2-amino-3-(5-methyl-3-oxo-1,2-oxazol-4-yl)propanoic acid receptor (AMPA)-mediated Ca^{2+} transients are significantly higher in cultured PMCA2^{+/-} PCs than in PMCA2^{+/+} PCs. This is due to increased Ca^{2+} influx, since P/Q type voltage-gated Ca^{2+} channel (VGCC) expression was more pronounced in PCs and cerebella of PMCA2^{+/-} mice and VGCC blockade prevented the elevation in amplitude. Neuronal nitric oxide synthase (nNOS) activity was higher in PMCA2^{+/-} cerebella and inhibition of nNOS or the soluble guanylate cyclase (sGC)-cyclic guanosine monophosphate (cGMP) pathway, which mediates nitric oxide (NO) signaling, reduced the amplitude of Ca^{2+} transients in PMCA2^{+/-} PCs, *in vitro*. In addition, there was an age-dependent decrease in metabotropic glutamate receptor 1 (mGluR1) and AMPA receptor subunit GluR2/3 transcript and protein levels at 8 weeks of age. These changes were followed by PC loss in the 20-week-old PMCA2^{+/-} mice. Our studies highlight the importance of PMCA2 in Ca^{2+} signaling, glutamate receptor expression and survival of Purkinje cells.

© 2012 Elsevier Inc. All rights reserved.

Introduction

Neuronal activity and survival are largely dependent on tightly regulated Ca^{2+} signaling. Intracellular Ca^{2+} ($[\text{Ca}^{2+}]_i$) homeostasis depends on multiple mechanisms including extrusion by ATP-dependent Ca^{2+}

pumps and the $\text{Na}^+/\text{Ca}^{2+}$ exchanger, intracellular sequestration into mitochondria, Golgi and the endoplasmic reticulum (ER), and buffering via Ca^{2+} binding proteins. In cerebellar PCs, the total rate of Ca^{2+} clearance relies considerably on the activity of plasma membrane Ca^{2+} ATPase isoform 2 (PMCA2), a high-affinity pump, most abundantly expressed in these cells (Burette et al., 2003; Marcos et al., 2009).

PMCA2 has been implicated in post-synaptic signaling in the cerebellum as well as the hippocampus as it is associated with synaptic signaling complexes (DeMarco and Strehler, 2001; Kurnellas et al., 2007; Sgambato-Faure et al., 2006). In the hippocampus, PMCA2w, a PMCA2 splice variant, is predominantly found at the post-synaptic density (PSD) in the dendritic spines (Burette et al., 2010). This localization suggests that PMCA2 is involved in the regulation of calcium signaling at the synapse via its association with synaptic molecular complexes. Similarly, immunoprecipitation studies with cerebellar extracts linked PMCA2 to mGluR1 and its downstream effectors, including the scaffolding protein Homer 3 and inositol 1,4,5-triphosphate (IP3R1) which mediates Ca^{2+}

Abbreviations: PMCA2, plasma membrane Ca^{2+} ATPase isoform 2; PC, Purkinje cell; mGluR1, metabotropic glutamate receptor 1; IP3R1, inositol 1,4,5-trisphosphate; SC, spinal cord; PSD, post synaptic density; AMPAR, α -amino-3-hydroxy-5-methyl-4-isoxazolepropionic acid receptor; VGCC, voltage gated Ca^{2+} channel; NO, nitric oxide; NOS, nitric oxide synthase; nNOS, neuronal nitric oxide synthase; eNOS, endothelial nitric oxide synthase; sGC, soluble guanylate cyclase; cGMP, cyclic guanosine monophosphate; ODO, 1H-[1,2,4]oxadiazolo[4,3-a]quinoxalin-1-one; 7-NINA, 7-nitro-indazole; CICR, Ca^{2+} induced Ca^{2+} release; RyR, ryanodine receptor; EAE, experimental autoimmune encephalomyelitis.

* Corresponding author at: Department of Neurological Surgery, UMDNJ-NJMS, 205 South Orange Avenue F-1204, Newark, NJ, 07103, USA. Fax: +1 973 972 1865.

E-mail address: elkabest@umdnj.edu (S. Elkabes).

release from the ER (Kurnellas et al., 2007). Subsequent investigations have shown an interaction between PMCA2, PSD-95 and N-Methyl-D-aspartate (NMDA) receptor subunits NR1 and NR2a, supporting the concept of interactions between PMCA2 and synaptic signaling complexes (Garside et al., 2009).

In the central nervous system (CNS), PMCA2 is predominantly expressed in neurons (Stauffer et al., 1995). The importance of this pump in the survival of brain and spinal cord neurons has been shown by RNA interference studies, *in vitro* (Fernandes et al., 2007; Garside et al., 2009; Kurnellas et al., 2010). The phenotype of PMCA2 heterozygous (PMCA2^{+/-}) and knockout mice also highlights the critical role of PMCA2 in CNS function and development (Kozel et al., 1998; Souayah et al., 2008). Even a partial reduction in PMCA2 in the heterozygous mice is sufficient to cause compromised noise-induced auditory responses and significant hearing loss occurring by 5–6 weeks of age (Kozel et al., 1998; Kozel et al., 2002). Delayed motor neuron loss in the spinal cord (SC) of these mice (Souayah et al., 2008) and depressed action potential firing in PCs of PMCA2^{+/-} mice have been reported (Empson et al., 2010).

The current studies defined molecular alterations observed in Purkinje cells of the PMCA2^{+/-} mice with particular emphasis on AMPAR-mediated Ca²⁺ signaling and glutamate receptor expression. Glutamate receptors and in particular, AMPAR were the focus of these investigations because they play a critical role in PC synaptic plasticity and function. This investigation provides insights into pathological mechanisms that affect PCs and the cerebellum.

Results

Ca²⁺ signaling in PMCA2^{+/-} PCs, *in vitro*

Enriched PC cultures were established from cerebella of PMCA2^{+/+} or PMCA2^{+/-} embryos and maintained 14 days *in vitro* (14 DIV). The decrease in PMCA2 expression in PMCA2^{+/-} cerebellum was confirmed by Western blot analysis (Figs. 1A–B). AMPAR-mediated Ca²⁺ transients were analyzed using Fura-2 Ca²⁺ imaging. Purkinje cells were identified by morphology during Ca²⁺ imaging and subsequently, their identity was corroborated by immunolabeling for calbindin, a PC marker. Co-localization of GluR2/3 with calbindin was confirmed by

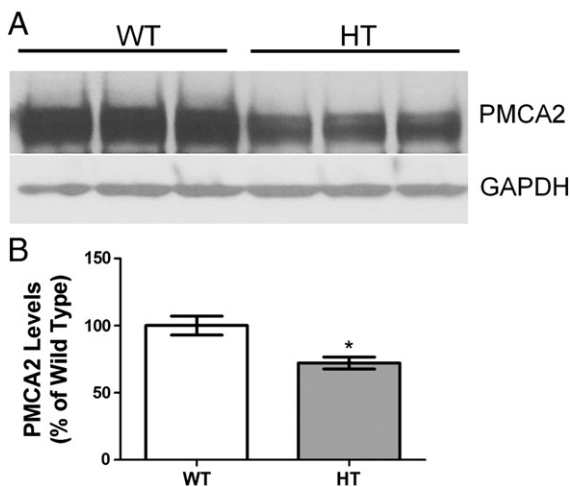


Fig. 1. PMCA2 levels in PMCA2^{+/+} and PMCA2^{+/-} cerebellum. (A) A representative Western blot showing a band at the appropriate molecular weight corresponding to PMCA2 (110 kDa) in protein extracts obtained from 3-week-old PMCA2^{+/+} (WT) and PMCA2^{+/-} (HT) mouse cerebellum (upper panel). The same blot was stripped and probed with an antibody against GAPDH, a housekeeping protein used to account for experimental variations (lower panel). (B) Quantification of Western blots after normalization to GAPDH. The graph shows the mean \pm S.E.M. of two independent experiments. Significantly different from WT **p* < 0.05 by *t*-test. N = 6 mice/group.

double-labeling (Fig. 2A). We used semi-quantitative immunocytochemistry (ICC) to measure GluR2/3 expression because the enriched PC cultures contain astrocytes, which also express GluR2/3 (Kovacs et al., 2002). Therefore, quantification at a single cell level was more suitable than another approach such as Western blotting which measures the combined expression in various cell subtypes present in the dish. These studies indicated no significant differences in GluR2/3 levels in PMCA2^{+/-} and PMCA2^{+/+} PCs, *in vitro* (Figs. 2B–C).

Subsequently, we studied AMPAR-mediated Ca²⁺ signaling. Stimulation of cultures with 3, 10 or 100 μ M AMPA (Figs. 3A–I) increased the amplitude of Ca²⁺ transients in PCs in a dose-dependent manner regardless of genotype. Ca²⁺ transient amplitudes were 1.6 fold higher in PMCA2^{+/-} mice than wild type controls at all concentrations examined (Table 1). This ceiling effect did not appear to be due to saturation of fura-2 Ca²⁺ signal, as application of KCl to cell cultures produced higher amplitude transients (results not shown). Decay time constants were also significantly higher in PMCA2^{+/-} PCs at every dose examined (Figs. 3A–I and Table 1).

To assess whether increased Ca²⁺ transient amplitudes in PMCA2^{+/-} PCs are due to altered Ca²⁺ influx via VGCCs, PCs were depolarized with potassium chloride (KCl; 130 mM), a stimulus which activates VGCCs. This evoked significantly larger Ca²⁺ transients in PMCA2^{+/-} PCs (363.2 \pm 30.5%) as compared to PMCA2^{+/+} PCs (240.1 \pm 18.8%; Figs. 4A–B), indicating that increases in Ca²⁺ transient amplitude are potentially due to increased Ca²⁺ influx via VGCCs. In agreement with this idea, semi-quantitative ICC on neurons with PC morphology indicated that P/Q-type VGCC expression in cultures derived from PMCA2^{+/-} cerebella is 50.7 \pm 9.4% higher than in the wild type cells (Figs. 4C–D). We corroborated this finding, *ex vivo*, by immunoblot analysis of the cerebellum in 3-week-old mice. We chose this age because the maturity of PCs, *in vivo*, at 3 weeks of age, corresponds to the maturity of PCs maintained 14 DIV (Gruol and Franklin, 1987; Hockberger et al., 1989). P/Q-type VGCC expression was significantly increased by 43.0 \pm 15.3% in PMCA2^{+/-} cerebella (Figs. 4E–F). Moreover, blockade of P/Q-type VGCCs with 200 nM ω -agatoxin TK decreased the amplitude of AMPAR-mediated Ca²⁺ transients in both PMCA2^{+/+} and PMCA2^{+/-} PCs (Fig. 4G). Thus, increased Ca²⁺ influx is most likely accountable for the elevated amplitude in PMCA2^{+/-} PCs.

Modulation of Ca²⁺ transient amplitudes by NO in PMCA2^{+/-} PCs

Nitric oxide is an intercellular messenger that has been implicated in Purkinje cell function (Lev-Ram et al., 2002; Marcoli et al., 2006; Namiki et al., 2005). We investigated the potential involvement of NO in the elevated AMPAR-mediated Ca²⁺ transient amplitudes in PMCA2^{+/-} PCs.

We first determined whether the activity of Ca²⁺-dependent forms of nitric oxide synthase (NOS) is increased in PMCA2^{+/-} cerebella. There was a 1.5-fold increase in neuronal NOS (nNOS) activity in PMCA2^{+/-} cerebella while no significant changes were observed in endothelial NOS (eNOS) activity (Figs. 5A–B).

Subsequently, we assessed whether short or long-term inhibition of nNOS activity by 7-NINA affects Ca²⁺ transient amplitudes in enriched PC cultures. To study the acute effects, PMCA2^{+/-} PC cultures were maintained 14 DIV and exposed to 5 μ M 7-NINA for 30 min, prior to AMPA stimulation. There were no changes in the amplitude of Ca²⁺ transients (not shown). Higher 7-NINA concentrations did not alter these results. To investigate chronic effects, 7-NINA was added to the cultures 7 days post-plating and AMPA-induced Ca²⁺ transients were evaluated at 14 days post-plating. This long-term treatment restored the amplitude of AMPAR-mediated Ca²⁺ transients to that of the vehicle-treated controls (Fig. 5C).

To assess whether activation of the soluble sGC-cGMP pathway is a mechanism mediating NO effects (Gallo and Iadecola, 2011), cultures were exposed chronically to 10 μ M 1 H-[1, 2,4]oxadiazolo[4,3-a]quinoxalin-1-one (ODQ), a sGC inhibitor. The amplitude of AMPAR-mediated Ca²⁺ transients in PMCA2^{+/-} PCs was restored to levels

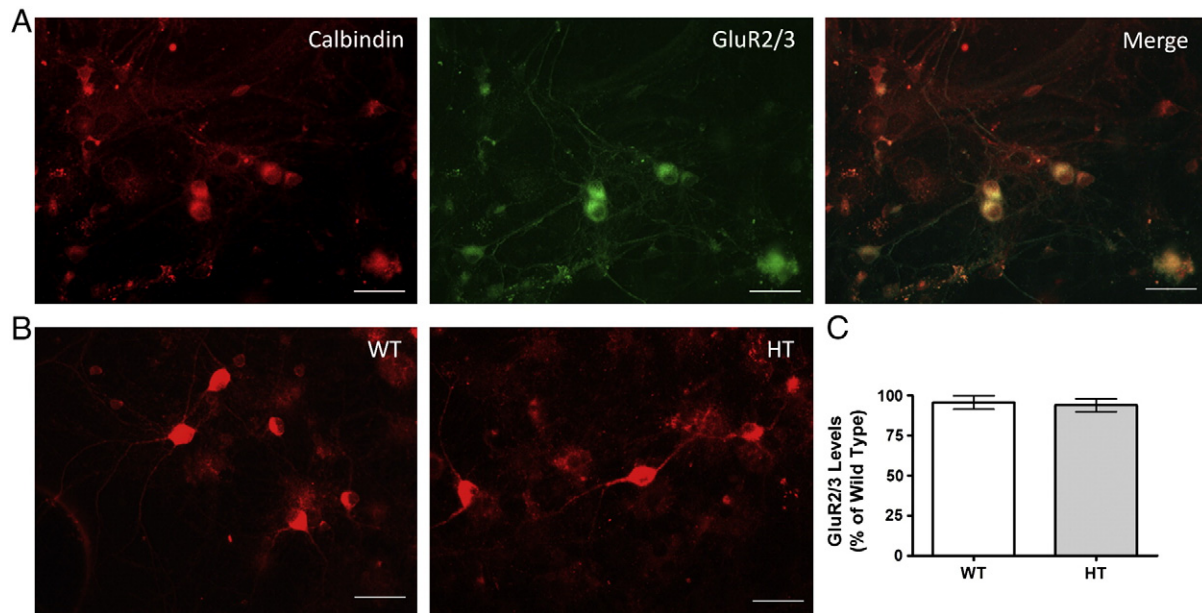


Fig. 2. Characterization of enriched PC cultures. (A) PCs maintained 14 DIV and immunolabeled for calbindin (left panel) and GluR2/3 (middle panel). The merged image demonstrates co-localization (right panel). (B) Representative PC cultures derived from PMCA2^{+/-} (HT) and PMCA2^{+/+} (WT) cerebella immunoreactive for GluR2/3. (C) Quantification of the GluR2/3 levels in PC cultures. There was no significant difference in the levels of GluR2/3 (PMCA2^{+/+}, n=68 cells/4 mice; PMCA2^{+/-}, n=86 cells/4 mice). Bar represents 30 μ m. The experiment was repeated twice and yielded similar results.

observed in PMCA2^{+/+} PCs (Fig. 5D). These results further support the notion that NO and its signaling pathway, sGC-cGMP, may be involved in the modulation of P/Q-type VGCCs in PMCA2^{+/-} PCs resulting in higher Ca²⁺ influx and elevated Ca²⁺ transient amplitudes.

Ca²⁺-binding proteins and intracellular Ca²⁺ release in PMCA2^{+/-} PCs

To determine the potential contribution of Ca²⁺ binding proteins to increased amplitudes of Ca²⁺ transients in PMCA2^{+/-} PCs, calbindin and parvalbumin levels were measured by semi-quantitative ICC. Calbindin levels were not significantly different in cultures derived from the PMCA2^{+/+} and PMCA2^{+/-} mice (Figs. 6A and C). In PMCA2^{+/-} PCs there was a significant 21.1 \pm 5.4% increase in parvalbumin levels (Figs. 6B and D). Immunoblots of 3-week-old cerebella indicated no significant differences in the level of either Ca²⁺ binding protein (Figs. 6E, F and G).

The possibility of Ca²⁺-induced-Ca²⁺ release (CICR) from the ER as a contributor to the higher amplitude was next analyzed. Increased cytosolic Ca²⁺ can activate ryanodine receptors (RyRs) in the ER resulting in the mobilization of internal Ca²⁺ stores, a phenomenon known as CICR. We first assessed whether activation of RyRs by exposure to 15 mM caffeine, elicits Ca²⁺ increase in enriched PC cultures from PMCA2^{+/-} or PMCA2^{+/+} mouse cerebellum (Womack et al., 2000). Caffeine stimulation produced no Ca²⁺ transients (Fig. 6H) in either culture types. This was not due to an overall aberrance in Ca²⁺ response as 130 mM KCl evoked a transient in the same cultures. A previous report has shown that in PCs, Ca²⁺ release from the endoplasmic reticulum occurs only when the internal stores are pre-loaded by exposure of cells to a depolarizing stimulus. If the cells are not exposed to KCl before they are challenged by caffeine, no Ca²⁺ transients are observed (Brorson et al., 1991). This latter finding is consistent with our results. Therefore, it is unlikely that release from internal Ca²⁺ stores contributes to the higher amplitudes in PMCA2^{+/-} PCs.

Age-dependent changes in glutamate receptor expression in the PMCA2^{+/-} mice

To determine whether decreases in PMCA2 expression affect glutamate receptor expression in PMCA2^{+/-} cerebella, we evaluated the protein levels of GluR2/3, mGluR1 and GluR δ 2, three glutamate receptors

important in PC synaptic plasticity (Aiba et al., 1994; Jeromin et al., 1996; Shigemoto et al., 1994; Steinberg et al., 2006). Initially, we analyzed glutamate receptors in the cerebellum of mice at 3 weeks post-natal, the age that corresponded to the maturity of PCs, *in vitro*, as indicated before. There were no significant changes in the levels of GluR2/3, mGluR1 and GluR δ 2 (Figs. 7A and B). Subsequently, we evaluated whether changes could occur at a later age. In fact, GluR2/3 and mGluR1 protein levels decreased by 29.3 \pm 9.5% and 29.3 \pm 6.0% respectively in PMCA2^{+/-} cerebella at 8 weeks of age (Figs. 7A and B). In contrast, no significant alterations were observed in GluR δ 2. As mentioned before, because GluR2/3 is also expressed in astrocytes, we performed studies to ascertain that the decrease in GluR2/3 occurs in PCs. We immunolabeled cerebellar sections obtained from the PMCA2^{+/+} and PMCA2^{+/-} mice and quantified GluR2/3 immunoreactivity in PCs (Fig. 7C). There was a small but significant decrease in GluR2/3 immunoreactivity in PMCA2^{+/-} PCs compared to PCs in PMCA2^{+/+} mice. To determine whether the decrease in mGluR1 and GluR2/3 was due to transcriptional regulation, we performed qRT-PCR. GluR2, GluR3 and mGluR1 transcript levels in PMCA2^{+/-} cerebella were decreased by 49.5 \pm 15.7%, 82.0 \pm 14.1% and 57.0 \pm 12.0% compared to the wild type, respectively, at 8 weeks of age (Fig. 7D). Thus, glutamate receptors undergo age-dependent reductions in expression in PMCA2^{+/-} cerebella.

Age-dependent changes in PC number in the cerebellum of PMCA2^{+/-} mice

We postulated that alterations in PMCA2 and glutamate receptor expression may cause PC pathology ultimately affecting PC survival. We quantified PC number, in identical regions of PMCA2^{+/-} and PMCA2^{+/+} cerebella at 8 and 20 weeks of age, using stereological cell counts. We also quantified the thickness of the molecular layer which contains PC dendrites, projecting axons and interneurons. There was no significant difference in PC number (Fig. 8A) or the thickness of the molecular layer (Fig. 8B) at 8 weeks of age. In contrast, by 20 weeks of age, there was a significant 17.8 \pm 7.6% reduction in PC number in PMCA2^{+/-} cerebella when compared to PMCA2^{+/+} cerebella (Fig. 8C). The thickness of the molecular layer remained unaltered (Fig. 8D).

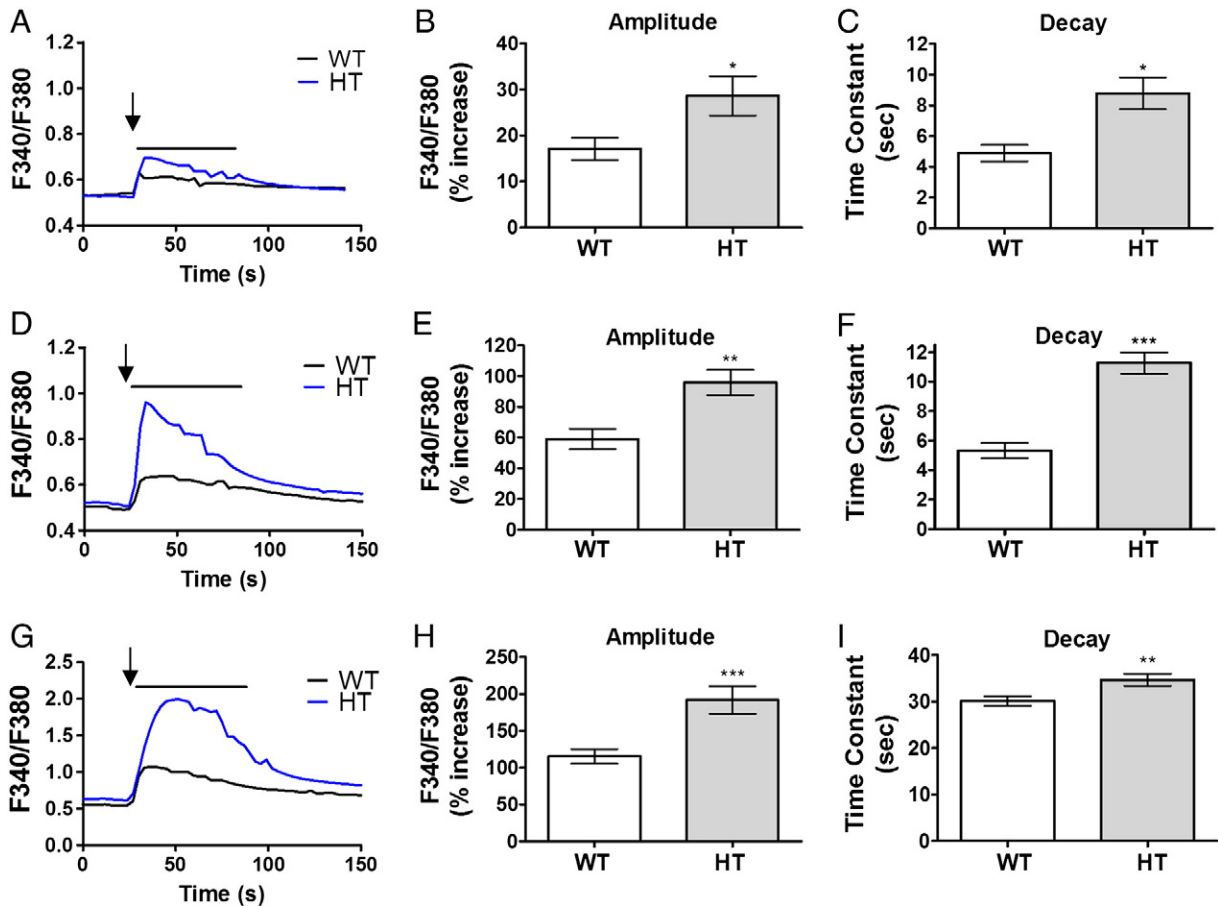


Fig. 3. The amplitude of AMPAR-mediated Ca^{2+} transients is increased in $\text{PMCA2}^{+/-}$ PCs, *in vitro*. (A) A representative trace showing the mean intracellular Ca^{2+} increase after stimulation of cells with 3 μM AMPA. Arrow indicates the time of AMPA application and bar indicates the duration of the treatment prior to the washout. (B and C) Quantification of Ca^{2+} transient amplitudes ($\text{PMCA2}^{+/+}$ $n=55$ cells/3 mice vs $\text{PMCA2}^{+/-}$ $n=96$ cells/3 mice) and decay time constants ($\text{PMCA2}^{+/+}$ $n=17$ cells/3 mice vs $\text{PMCA2}^{+/-}$ $n=34$ cells/3 mice), respectively, after application of 3 μM AMPA. (D) A representative trace showing the mean intracellular Ca^{2+} increase after stimulation with 10 μM AMPA. (E and F) Quantification of Ca^{2+} transient amplitudes ($\text{PMCA2}^{+/+}$ $n=56$ cells/3 mice vs $\text{PMCA2}^{+/-}$ $n=98$ cells/3 mice) and decay time constants ($\text{PMCA2}^{+/+}$ $n=54$ cells/3 mice vs $\text{PMCA2}^{+/-}$ $n=93$ cells/3 mice), respectively, after application of 10 μM AMPA. (G) A representative trace showing the mean intracellular Ca^{2+} increase after stimulation with 100 μM AMPA. (H and I) Quantification Ca^{2+} transient amplitudes ($\text{PMCA2}^{+/+}$ $n=144$ cell/12 mice vs $\text{PMCA2}^{+/-}$ $n=170$ cells/13 mice) and decay time constants ($\text{PMCA2}^{+/+}$ $n=118$ cells/12 mice vs $\text{PMCA2}^{+/-}$ $n=102$ cells/13 mice), respectively, after application of 100 μM AMPA. Each treatment was repeated 2–3 times. Statistically significant by unpaired *t*-test, * $p<0.05$, ** $p<0.001$, *** $p<0.0001$.

Discussion

The current studies used $\text{PMCA2}^{+/-}$ mice as a model, to unravel mechanisms by which reductions in PMCA2 levels result in altered Ca^{2+} signaling in PCs. Based on a combination of ex-vivo and *in vitro* investigations, we propose that increased Ca^{2+} influx, as a result of enhancement in P/Q-type VGCC expression lead to higher Ca^{2+} transient amplitudes in $\text{PMCA2}^{+/-}$ PCs in response to a depolarizing stimulus or AMPAR activation. As Ca^{2+} influx through P/Q-type VGCCs activates K^+ channels that hyperpolarize neurons (Womack and Khodakhah, 2003; Womack et al., 2004), increased influx could decrease action potential frequency in $\text{PMCA2}^{+/-}$ PCs. In fact, depressed spontaneous action potential

frequency in $\text{PMCA2}^{+/-}$ PCs has been reported (Empson et al., 2010). Such perturbations could disrupt the relay of information from PCs to other neurons leading to neural dysfunction.

Our investigations indicated higher nNOS activity in the cerebellum of $\text{PMCA2}^{+/-}$ mice, compared to wild type littermates suggesting higher NO production. We also found that inhibition of nNOS activity in enriched PC cultures abolishes the differences in Ca^{2+} -transient amplitudes between $\text{PMCA2}^{+/-}$ and $\text{PMCA2}^{+/+}$ PCs, *in vitro*. In the cerebellum, nNOS immunoreactivity is not found in PCs but is localized to the molecular layer (Gotti et al., 2005; Suarez et al., 2005). Thus, both afferent fibers that project on PC dendrites (Shibuki and Kimura, 1997) and interneurons (Shin and Linden, 2005) could be releasing NO. It is likely that in our enriched PC cultures, interneurons are the principal source of NO. Previous studies have shown that nitric oxide can modulate protein expression (Lee et al., 2010; Ota et al., 2010). In addition, NO may acutely affect Ca^{2+} influx by oxidizing P/Q-type VGCCs (Chen et al., 2002). It is possible that such mechanisms underlie the changes in VGCC expression and Ca^{2+} influx.

The sGC-cGMP pathway is the physiological mediator of NO effects. In fact, inhibition of sGC prevents the differences in Ca^{2+} transient amplitudes between $\text{PMCA2}^{+/-}$ and $\text{PMCA2}^{+/+}$ PCs. These results, taken together, suggest that PCs in the $\text{PMCA2}^{+/-}$ cerebellum could be exposed to higher NO than in the cerebellum of the wild type mouse. As NO is an important contributor to PC signaling and function (Lev-Ram et al,

Table 1

Ca^{2+} transient amplitude and decay time constant in $\text{PMCA2}^{+/+}$ and $\text{PMCA2}^{+/-}$ PCs in response to AMPA. The increase in amplitude is expressed as percent increase in the ratio of F340/F380 over baseline ratio (also see Fig. 3).

	Ca^{2+} transient amplitude (% increase)		Decay time constant (s)	
	$\text{PMCA2}^{+/+}$	$\text{PMCA2}^{+/-}$	$\text{PMCA2}^{+/+}$	$\text{PMCA2}^{+/-}$
AMPA 3 μM	17.1 \pm 2.4	28.6 \pm 4.3	4.9 \pm 0.5	8.8 \pm 1.0
AMPA 10 μM	59.1 \pm 6.6	95.9 \pm 8.3	5.3 \pm 0.51	11.3 \pm 0.72
AMPA 100 μM	115.4 \pm 9.7	191.9 \pm 18.7	30.1 \pm 1.0	34.7 \pm 1.3

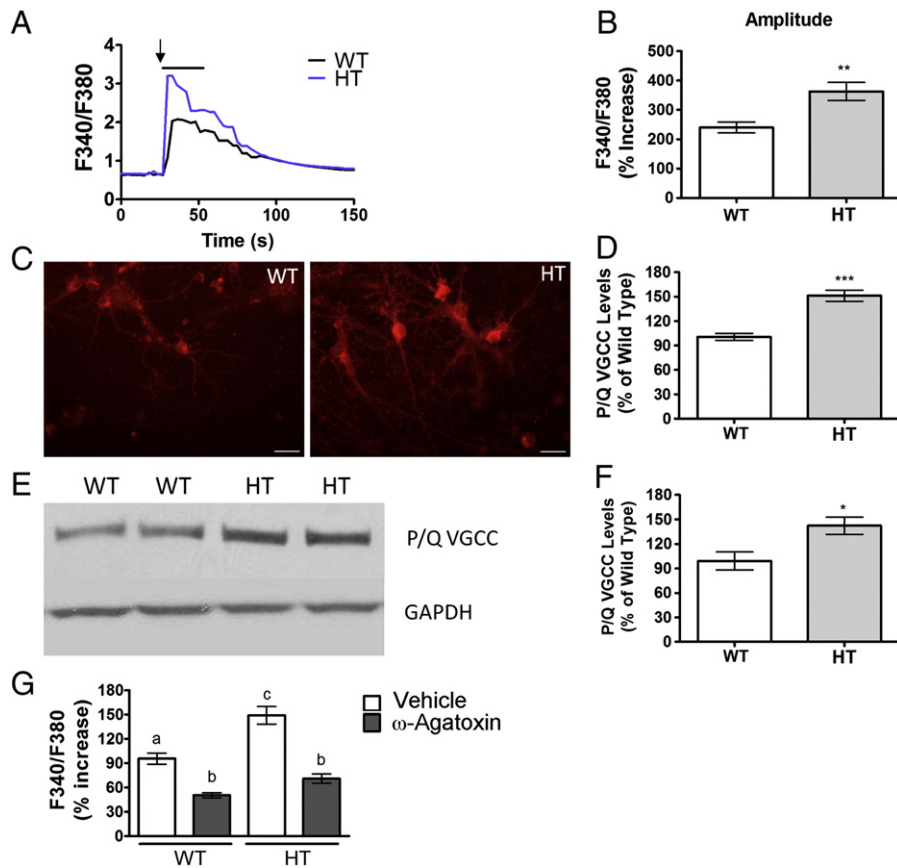


Fig. 4. The expression of P/Q type VGCCs is increased in the cerebellum and enriched PC cultures of PMCA2^{+/-} (HT) mice. (A) The trace showing the mean intracellular Ca²⁺ response after stimulation of cultures with 130 mM KCl. Arrow indicates application of KCl and the bar represents the washout period. (B) Quantification of Ca²⁺ transient amplitudes in KCl stimulated PCs (PMCA2^{+/+} n = 65 cells/7 mice vs PMCA2^{+/-} n = 130 cells/8 mice; Significantly different from the wild type (WT) by unpaired *t*-test; ***p* < 0.001). (C) Representative PCs maintained 14 DIV and immunolabeled for P/Q-type VGCCs. Bar represents 30 μm. (D) Quantification of the P/Q-type VGCC immunoreactivity in PMCA2^{+/+} (WT) and PMCA2^{+/-} (HT) PCs. There was an increase in P/Q-type VGCC levels in PCs of PMCA2^{+/-} mice (PMCA2^{+/+} n = 36 cells/4 mice vs PMCA2^{+/-} n = 59 cells/4 mice. Significantly different from WT by unpaired *t*-test, ****p* < 0.0001). (E) Representative Western blot probed for P/Q-type VGCCs in 3-week-old PMCA2^{+/-} and PMCA2^{+/+} mouse cerebellum. (F) Quantification of Western blots shown in E. There was a 43.0 ± 15.3% increase in VGCC levels in PMCA2^{+/-} mice when compared with PMCA2^{+/+} controls (Significantly different from WT by unpaired *t*-test, **p* < 0.05, n = 6 cerebella/group). (G) Inhibition of AMPAR-induced (100 μM AMPA) [Ca²⁺]_i increases by 200 nM ω-agatoxin TK. (PMCA2^{+/+}; n = 128 cells/6 mice and PMCA2^{+/-}; n = 106 cells/5 mice. a = significantly different from c, b = significantly different from a and c by one-way ANOVA *p* < 0.0001, Bonferroni's post-hoc test). The experiments were repeated twice and yielded similar results.

2002; Marcoli et al., 2006; Namiki et al., 2005) exposure of PCs to excess NO, either released by parallel fibers or by interneurons, can cause defective PC function and signaling in PMCA2^{+/-} cerebellum.

In addition, we found an age dependent-reduction in mGluR1 and GluR2/3 expression in the cerebellum of the PMCA2-heterozygous mice as compared to the wild type. Both AMPAR and mGluR1 are important in cerebellar function including PC synaptic plasticity (Aiba et al., 1994; Shigemoto et al., 1994; Steinberg et al., 2006). Moreover, it is worth noting that glutamate receptors are spatially clustered with VGCCs (Froehner, 1993; Klemmer et al., 2009) and in the cerebellum, stimulation of mGluR1 modulates the activity of P/Q-type VGCCs via direct interactions (Kitano et al., 2003). It is possible to speculate that such interactions are perturbed in the cerebellum of the PMCA2^{+/-} mice. It would be interesting to determine whether the PMCA2-heterozygous mice develop age-dependent functional deficits attributable to progressive cerebellar dysfunction that parallels the observed molecular changes. However, such studies are hampered by the fact that an overall reduction in PMCA2 expression in the heterozygous mice affects not only the cerebellum but also other CNS regions confounding the evaluation of cerebellum-related deficits. Therefore, the future development of conditional knockout mice, which can allow the selective deletion of PMCA2 in PCs, could shed insights into the contribution of PMCA2 to cerebellar function and dysfunction.

The culmination of the molecular alterations reported here could cause PC dysfunction. We also observed delayed PC loss in the 20-week-old PMCA2^{+/-} mice. It is worth noting that we have previously

reported delayed neuronal loss in another CNS region of the PMCA2^{+/-} mice: the number of motor neurons in the ventral horn of the PMCA2^{+/-} mouse spinal cord decreases as the animal ages (Souayah et al., 2008). These findings highlight the importance of PMCA2 in the survival of some neuronal populations. We conclude that partial reductions in PMCA2 levels could be sufficient to perturb the function and integrity of select neuronal populations and the overall outcome on cell survival may manifest itself in a delayed fashion.

PMCA2s and in particular, PMCA2, have been implicated in human disorders and animal models of human diseases. Of special interest to the current study is a recent report showing a genetic variance in the 3p25 region containing the PMCA2 gene, ATP2B2, in male autistic subjects (Carayol et al., 2011). Autism is a developmental disorder that is manifested by poor communication and social skills and stereotyped behaviors. A decrease in the number of PCs is an anatomical abnormality identified in autistic individuals (Bauman and Kemper, 2005). In our PMCA2^{+/-} model, the dysregulation of Ca²⁺ signaling and the perturbations in glutamate receptor signaling complexes are paralleled by delayed PC loss. It is possible to contemplate that the mechanisms described here may be relevant to PC dysfunction and loss that occurs in autistic individuals.

Reductions in PMCA2 in other CNS regions have also been implicated in neuronal loss in animal models of human diseases. In experimental autoimmune encephalomyelitis (EAE), an animal model of MS, reduced PMCA2 levels in the lumbar spinal cord coincide with disease onset (Nicot et al., 2003). The decrease in PMCA2 is believed to occur

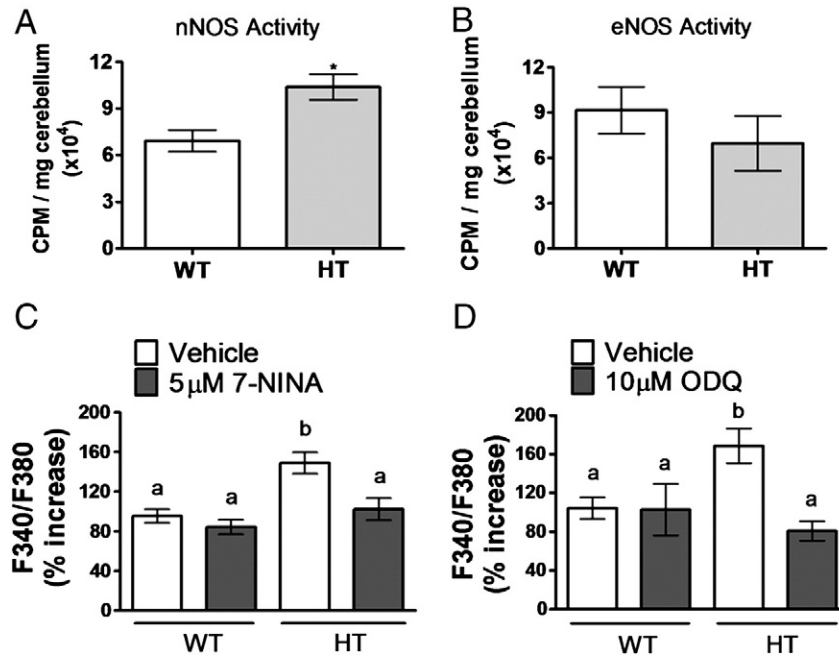


Fig. 5. nNOS activity in the cerebellum of PMCA2^{+/+} (WT) and PMCA2^{+/-} (HT) mice. (A and B) Quantification of specific nNOS and eNOS activity (Significantly different from WT by unpaired *t*-test **p*<0.05, *n*=4–5 mice/group). (C) Restoration of AMPAR-mediated (100 μM AMPA) Ca²⁺ transient amplitude in PMCA2^{+/-} PCs after treatment with 5 μM 7-NINA for 7 days (PMCA2^{+/+}: vehicle *n*=128 cells/6 mice vs 5 μM 7-NINA *n*=129 cells/6 mice; PMCA2^{+/-}: vehicle *n*=106 cells/5 mice vs 5 μM 7-NINA *n*=86 cells/5 mice. *b*=significantly different from *a* by one-way ANOVA *p*<0.0001, Bonferroni's post-hoc test). (D). Restoration of AMPAR-mediated (100 μM AMPA) Ca²⁺ transient amplitude in PMCA2^{+/-} PCs after treatment with 10 μM ODQ for 7 days (PMCA2^{+/+}: vehicle *n*=36 cells/3 mice vs 10 μM ODQ *n*=16 cells/3 mice; PMCA2^{+/-}: vehicle *n*=55 cells/5 mice vs 10 μM ODQ *n*=41 cells/5 mice). The results were analyzed by one-way ANOVA, (Bonferroni's post-hoc test), *b*=significantly different from *a*, *p*<0.0001. The experiment was repeated twice and yielded similar results.

downstream to glutamate excitotoxicity as treatment with an AMPA/kainate receptor antagonist restores PMCA2 levels (Xu et al., 2007) and direct exposure of spinal cord neurons to kainic acid, *in vitro*, reduces PMCA2 levels via calpain-mediated degradation (Kurnellas et al., 2010). In agreement with these findings, *in vivo* administration of kainic acid to the hippocampus, decreases PMCA2 expression (Garcia et al., 1997) whereas NMDA receptor activation triggers PMCA2 internalization and calpain-mediated degradation (Pottorf et al., 2006). In addition, PMCA2 mutations have been associated with deafness in mice (Bortolozzi et al., 2010; Spiden et al., 2008; Prasad et al., 2007).

In summary, our studies highlight the importance of PMCA2 in PCs: Changes in Ca²⁺ handling and decreases in the expression of essential glutamate receptors are observed when PMCA2 levels are reduced. In addition, delayed PC death occurs when PMCA2 levels are reduced continuously.

Experimental methods

Animals

Black Swiss PMCA2^{+/-} and PMCA2^{+/+} mice of either gender, were housed in the Comparative Medicine Resources facility at New Jersey Medical School (NJMS) on a 12:12 h light–dark cycle at 22–23 °C with water and standard chow provided *ab libitum*. All procedures were approved by the NJMS Institutional Animal Care and Use Committee.

Enriched PC cultures

Cerebellum from embryonic day 17 (E17) PMCA2^{+/-} and PMCA2^{+/+} mice were dissociated with trypsin (0.1%), resuspended in DNase (0.05%) and triturated. The cells obtained from each cerebellum were plated individually in 10 × 10 mm cloning cylinders on 25 mm polyornithine-coated cover slips (6–12 cloning cylinders per embryo), at a density of

3.2 × 10⁵ cells/cm², in plating media (DMEM/F-12 media with 10% FBS and 10 μg/ml gentamicin) for 24 h. Media were replaced with DMEM/F-12 supplemented with progesterone (0.5 μM), putrescine (100 μM), sodium selenite (30 nM), insulin (0.01 mg/ml), transferrin (0.1 mg/ml) and bovine serum albumin (BSA; 100 μg/ml). Cultures were maintained at 37 °C, 100% humidity and 5% CO₂/O₂ mix for 14 days *in vitro* (DIV) to allow for PC maturation. A tissue sample from each embryo was processed to determine the genotype. Cultures were enriched in PCs but contained glia and other small diameter neuronal subtypes.

Fura-2 Ca²⁺ imaging

Enriched PC cultures maintained 14 DIV were loaded with Fura-2/acetoxymethyl ester (5 μM; Molecular Probes, Eugene, OR) by incubating the cells in a physiological recording buffer (in mM: 0.5 Na₂HPO₄, 0.5 NaH₂PO₄, 120 NaCl, 5 KCl, 25 HEPES, 1.0 CaCl₂, 0.3 MgCl₂, 7 NaHCO₃, 0.4 MgSO₄, and 5 glucose with 0.25% fatty acid free BSA) supplemented with pluronic acid (0.02%) for 30 min at 37 °C under gentle agitation. Cells were washed three times, then transferred to a thermostatically regulated microscope chamber (37 °C) on a Nikon Diaphot inverted microscope (Nikon, Melville, NY). Fura-2 fluorescence images from PC cell bodies identified by their large diameter and distinct dendritic morphology (excitation, 340 and 380 nm, emission 420–600 nm) were acquired every 3 s with a cooled charged coupled camera. Ratio Ca²⁺ measurements were calculated after background subtraction and autofluorescence correction using customized software. Decay time constants were determined in Sigma Plot 8.0 (Systat Software, Point Richmond, CA), by fitting the decaying phase of the Ca²⁺ transient with a single exponential.

Responses were elicited by the addition of either 3 μM, 10 μM, 100 μM AMPA (Tocris, Ellisville, MO), 15 mM caffeine or 130 mM potassium chloride (KCl) followed by a washout of the stimulant. In some experiments, PCs treated with 200 nM ω-agatoxin TK (30 min; Tocris), 5 μM 7-Nitroindazole monosodium salt (7-NINA, Tocris), 10 μM

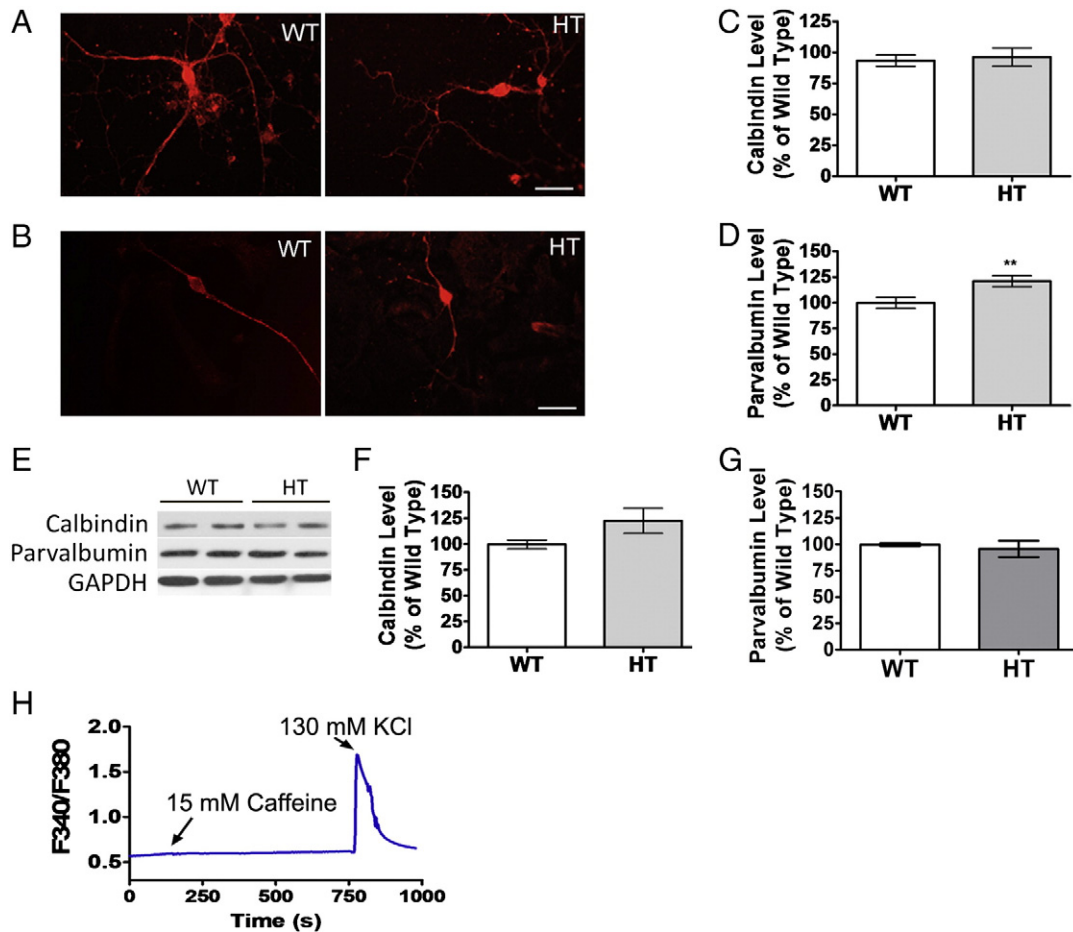


Fig. 6. Calcium binding proteins calbindin and parvalbumin and endoplasmic reticulum Ca^{2+} release do not contribute to the increased amplitude of Ca^{2+} transients in $\text{PMCA2}^{+/-}$ PCs. (A and B) Representative PCs grown in culture for 14 DIV stained for calbindin (A) and parvalbumin (B). Bar represents 30 μm . (C and D) Quantification of calbindin and parvalbumin immunoreactivity. There was no significant difference in calbindin level ($\text{PMCA2}^{+/+}$ $n=86$ cells/4 mice; $\text{PMCA2}^{+/-}$ $n=55$ cells/3 mice). Parvalbumin level showed a small increase in $\text{PMCA2}^{+/-}$ PCs compared to $\text{PMCA2}^{+/+}$ PCs ($\text{PMCA2}^{+/-}$ $n=73$ cells/3 mice vs $\text{PMCA2}^{+/+}$ $n=68$ cells/3 mice; significantly different from WT by unpaired t -test, $**p<0.001$). (E) A representative Western blot showing calbindin and parvalbumin expression in $\text{PMCA2}^{+/-}$ and $\text{PMCA2}^{+/+}$ mouse cerebella at 3 weeks of age. (F–G) Quantification of Western blots shown in (E). There were no significant differences in the levels of either protein ($n=6/\text{group}$). (H) Representative trace following stimulation of cultured PCs with 15 mM caffeine. Note that caffeine does not evoke a calcium transient. Each experiment was repeated twice and yielded similar results.

1 H-[1,2,4]oxadiazolo[4,3-a]quinoxalin-1-one (ODQ, Tocris) or vehicle before stimulation with 100 μM AMPA. For each separate treatment, naive PC cultures were used except where 100 μM AMPA Ca^{2+} transients were compared before and after treatment with ω -agatoxin TK. One coverslip from each individual embryo in the litter was used in imaging experiments and all the PCs in field were analyzed individually.

Immunocytochemistry

Enriched PC cultures maintained 14 DIV were fixed in 4% paraformaldehyde in 0.1 M phosphate buffer pH 7.4 and incubated with antibodies against GluR2/3 (1:1000; Millipore, Danvers, MA), P/Q-type VGCC (1:100; Sigma, St. Louis, MO), parvalbumin (1:4000; Millipore) or calbindin D-28k (1:1000; Millipore) for 18 h at 4 $^{\circ}\text{C}$. Signals were visualized using respective biotinylated secondary antibodies (1:500; Vector, Burlingame, CA) or Alexa Fluor 488 labeled anti-rabbit IgG (1:100; Vector) for 60 min at room temperature. Samples incubated with biotinylated secondary antibodies were exposed to Texas Red Avidin D (Vector) for 20 min, washed and mounted using Vectashield (Vector). Immunoreactive cells were visualized on an upright fluorescence microscope (Leica DM5500B, Wetzlar, Germany). Individual cell bodies were outlined on grayscale images and mean gray value was measured using ImageJ software. On each coverslip the mean gray value of three

background regions was measured and the average background intensity was subtracted from each value. Densitometry/image analysis was performed using ImageJ software.

Immunoblotting

Whole cerebella from 3, 8 and 20-week-old $\text{PMCA2}^{+/-}$ and $\text{PMCA2}^{+/+}$ mice were homogenized in lysis buffer (in mM; 10 HEPES pH 8.0, 150 NaCl, 50 NaF, 0.2 PMSF and 0.1% sodium dodecylsulfate, 1% NP40, 0.5% deoxycholic acid as well as 2 $\mu\text{g}/\text{ml}$ pepstatin A, aprotinin and leupeptin). Membrane bound proteins were solubilized by three repeated freeze/thaw cycles at $-140^{\circ}\text{C}/37^{\circ}\text{C}$. Proteins were resolved on 3–8% Tris Acetate or 10% Bis-Tris gels (Invitrogen) and transferred to PVDF membranes (Invitrogen). Membranes were probed with antibodies against mGluR1 (1:2500; BD Biosciences, Sparks, MD), GluR2/3 (1:1000; Millipore), P/Q-type VGCC (1:500; Sigma), calbindin (1:2500; Millipore), parvalbumin (1:3000; Millipore), GluR δ 1/2 (1:5000; Millipore) and GAPDH as an endogenous control (1:10,000; EMD Chemicals, Gibbstown, NJ) overnight at 4 $^{\circ}\text{C}$. Signals were visualized using respective secondary antibodies (Jackson ImmunoResearch, West Grove, PA) and Pierce ECL Western blotting substrate (ThermoFisher, Rockford, IL) and by exposure to autoradiography film. Densitometry was performed using Un-Scan-It software (Silk Scientific, Orem, Utah).

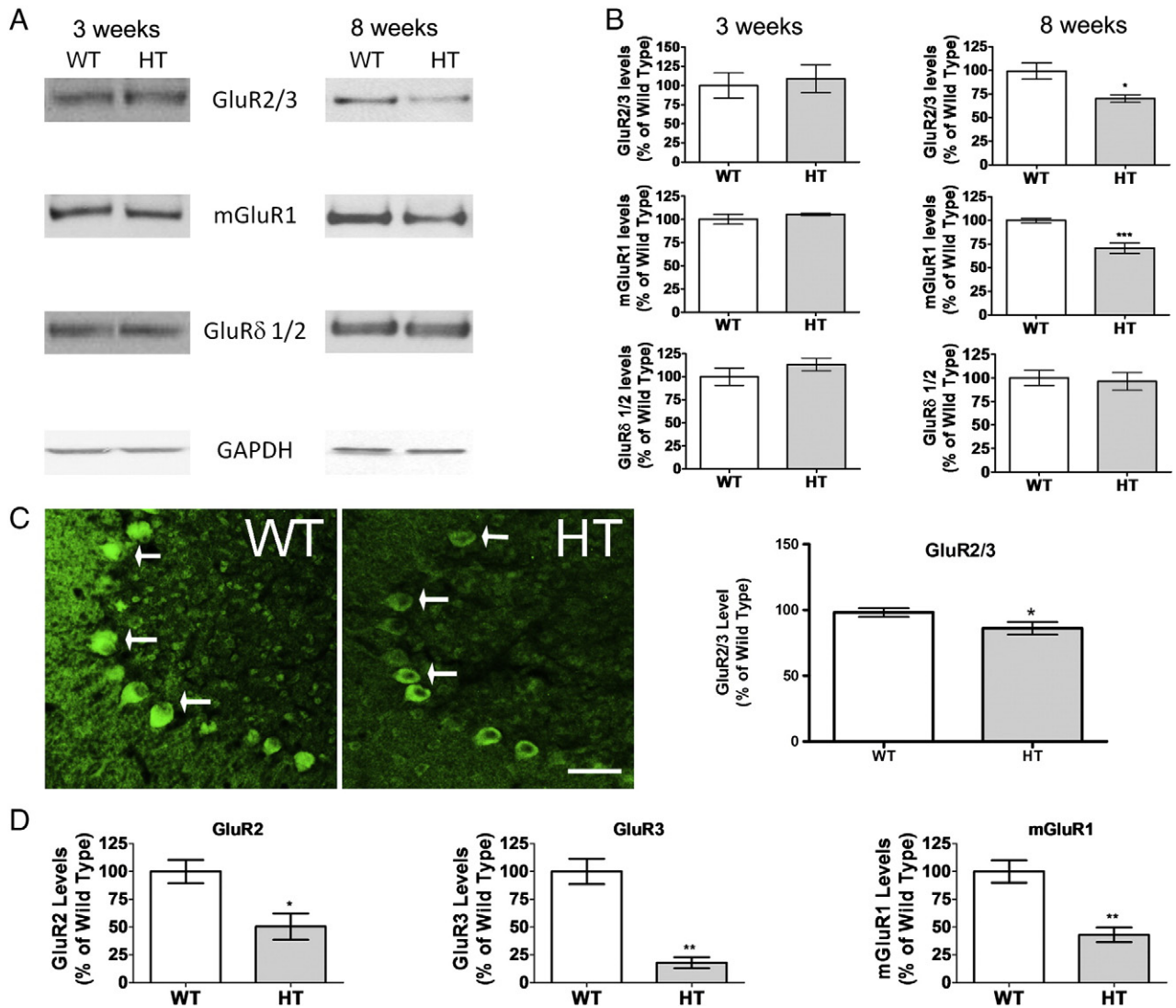


Fig. 7. Expression of glutamate receptors in $PMCA2^{+/-}$ cerebellum at 3 and 8 weeks of age. (A) Representative Western blots showing a band at the appropriate molecular weight corresponding to GluR2/3 (110 kDa), mGluR1 (133 kDa), GluR δ 2 (114 kDa) in 3- and 8-week-old $PMCA2^{+/-}$ (HT) and $PMCA2^{+/+}$ (WT) mice. (B) Quantification of Western blots shown in A. There was no significant difference in glutamate receptor levels at 3 weeks of age. Levels of GluR2/3 and mGluR1 were lower in $PMCA2^{+/-}$ cerebellum by 8 week of age. Significantly different from WT by unpaired *t*-test, * $p < 0.05$, ** $p < 0.001$, *** $p < 0.0001$, $n = 4$ /group. $n = 6$ /group. The experiment was repeated 3 times and yielded similar results. (C) Two photomicrographs showing GluR2/3 immunoreactive PCs in the wild type (WT) and $PMCA2^{+/-}$ (HT) mice. Arrows point to labeled PCs. Bar represents 30 μ m (left panel). The graph on the right panel is the quantification of the signal in individual PCs. $n = 33 - 35$ cells/group * $p < 0.05$ by unpaired *t*-test. (D) Quantification of GluR2, GluR3 and mGluR1 transcript levels by real time RT-PCR at 8 weeks of age. Significantly different from wild type * $p < 0.05$, ** $p < 0.001$, * $n = 4$ /group.

Quantitative RT-PCR

Total cellular RNA from 8-week-old $PMCA^{+/-}$ and $PMCA^{+/+}$ mouse cerebella was extracted using TRIzol reagent (Invitrogen) and the RNeasy Midi kit (QIAGEN, Valencia, CA) followed by reverse transcription using the Superscript III First Strand cDNA Synthesis kit (Invitrogen) according to the manufacturer's instructions. Quantitative RT-PCR reactions (20 μ l) were prepared with 50 ng cDNA in DEPC-treated water, 10 μ l of 2 \times TaqMan Universal PCR Master Mix (Applied Biosystems) and 1 μ l of the respective probes (TaqMan Gene Expression Assays, mGluR1 (Mm00810231.s1), GluR2 (Mm00442822.m1), GluR3 (Mm00497517.m1) Applied Biosystems). Reactions were amplified with a RealPlex 4 Cycler (Eppendorf, Hauppauge, NY). The mixture was heated for 2 min at 50 $^{\circ}$ C, followed by 95 $^{\circ}$ C for 10 min. Denaturation was at 95 $^{\circ}$ C for 15 s and annealing/extension at 60 $^{\circ}$ C for 1 min. The reaction was performed for 40 cycles. To verify the specificity of the amplification reaction, melting-curve analysis was performed. 18S mRNA (Applied Biosystems, Hs03003631.q1) was used for normalization. The threshold cycle (CT) value was taken as

the fractional cycle number at which the emitted fluorescence of the sample passes a fixed threshold above the baseline. The modified 2CT method was used to calculate the relative differences between $PMCA^{+/-}$ and $PMCA^{+/+}$ groups as a fold change in gene expression.

Stereological analysis and anatomical measurements

Eight and 20-week-old $PMCA^{+/-}$ and $PMCA^{+/+}$ mice were perfused with 4% paraformaldehyde in 0.1 M phosphate buffer pH 7.4. The cerebella were removed and postfixed. Fifty- μ m thick parasagittal sections were obtained using a vibratome (Leica VT1200) and mounted on slides. After Nissl staining the average thickness of the sections was 22.2 μ m. Stereology was performed using the optical fractionator method (Stereo Investigator version 7.0; MicroBrightField, Colchester, VT) on a microscope with an x-, y-, z-axis motorized stage (Bio Point 30; Ludl Electronic Products, Hawthorne, NY). Leading edges of Nissl stained PC cell bodies in lobules 4 and 5 of the PC layer in every sixth section were counted using a 40 \times objective lens (NeoFluar, 0.75 NA; Zeiss, Oberkochen, Germany). Cells in the uppermost focal plane (2 μ m) were not counted. The

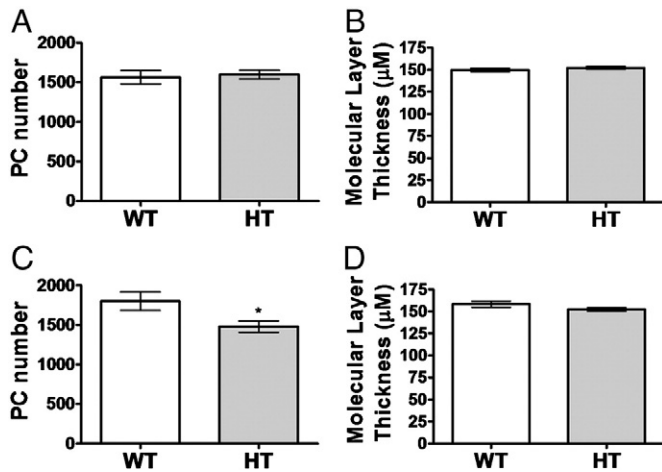


Fig. 8. Decreased Purkinje cell number at 20 weeks of age. (A–B) Purkinje cell number and molecular layer thickness are not significantly different at 8 weeks of age in $PMCA2^{+/-}$ (HT) mice when compared with $PMCA2^{+/+}$ (WT) mice. (C–D) At 20 weeks of age, there is a reduction in PC number in $PMCA2^{+/-}$ mice but no significant change in the thickness of the molecular layer. Significantly different from WT by unpaired *t*-test, * $p < 0.05$, $n = 5$ /group. The experiment was repeated 3 times and yielded similar results.

counting frame had a height of 15 μm and was 75 $\mu\text{m} \times 75 \mu\text{m}$ in size and the sampling grid was 50 $\mu\text{m} \times 50 \mu\text{m}$. Using these parameters approximately 300 markers were counted per cerebellum. The thickness of the molecular layer was measured on the same sections used for stereological cell counts (NeuroLucida; MicroBrightField).

NOS activity

NOS activity was measured using a radiodetection kit (EMD Biosciences, San Diego, CA) based on the conversion of (^3H) L-arginine to (^3H) L-citrulline. Cerebellar homogenates were prepared from 3-week-old $PMCA2^{+/+}$ and $PMCA2^{+/-}$ cerebellum as described by the manufacturer. nNOS, activity was measured in homogenates exposed to 10 μM eNOS inhibitor, N^5 -(1-Iminoethyl)-L-ornithine dihydrochloride (L-NIO, Sigma Aldrich, St. Louis, MO) and eNOS activity was measured in the presence of 10 μM nNOS inhibitor 7-NINA. Experiments were performed in the presence of saturating levels of Ca^{2+} (250 μM) to measure Ca^{2+} dependent forms of NOS. Radiolabeled (^3H) L-arginine was obtained from Perkin Elmer.

Statistical analysis

Values are represented as average \pm S.E.M. To calculate percent of wild type, values obtained from the wild type samples were averaged. All values for wild type and heterozygous samples were individually normalized to this average to calculate S.E.M. Data were analyzed with GraphPad v4.03 (Graphpad Software, La Jolla, CA) using Student's *t*-test or one-way ANOVA followed by Bonferroni's *post-hoc* Test. $p < 0.05$ was considered statistically significant.

Acknowledgments

We thank Drs. Vanessa Routh, Joseph McArdle, Michael P. Kurnellas, Amanda Craig and Kevin Pang for valuable help and advice with some of the experiments. We are grateful to Dr. Arnaud Nicot for carefully reading the manuscript. The authors wish to acknowledge their appreciation to Dr. Robert F. Heary and The Reynolds Family Spine Laboratory members. This work was generously supported by grants NS046363 from NIH-NINDS and UMDNJ Foundation to SE and NIH grant NS046593 to HL. AKF was partly supported by T32 5T32NS051157 from NIH. The authors declare no conflict of interest.

References

- Aiba, A., Kano, M., Chen, C., Stanton, M.E., Fox, G.D., Herrup, K., Zwingman, T.A., Tonegawa, S., 1994. Deficient cerebellar long-term depression and impaired motor learning in mGluR1 mutant mice. *Cell* 79, 377–388.
- Bauman, M.L., Kemper, T.L., 2005. Neuroanatomic observations of the brain in autism: a review and future directions. *Int. J. Dev. Neurosci.* 23, 183–187.
- Bortolozzi, M., Brini, M., Parkinson, N., Crispino, G., Scimemi, P., De Siati, R.D., Di Leva, F., Parker, A., Ortolano, S., Arsan, E., Brown, S.D., Carafoli, E., Mammano, F., 2010. The novel $PMCA2$ pump mutation Tommy impairs cytosolic calcium clearance in hair cells and links to deafness in mice. *J. Biol. Chem.* 285, 37693–37703.
- Bronson, J.R., Bleakman, D., Gibbons, S.J., Miller, R.J., 1991. The properties of intracellular calcium stores in cultured rat cerebellar neurons. *J. Neurosci.* 11, 4024–4043.
- Burette, A., Rockwood, J.M., Strehler, E.E., Weinberg, R.J., 2003. Isoform-specific distribution of the plasma membrane Ca^{2+} ATPase in the rat brain. *J. Comp. Neurol.* 467, 464–476.
- Burette, A.C., Strehler, E.E., Weinberg, R.J., 2010. A plasma membrane Ca^{2+} ATPase isoform at the postsynaptic density. *Neuroscience* 169, 987–993.
- Carayol, J., Sacco, R., Tores, F., Rousseau, F., Lewin, P., Hager, J., Persico, A.M., 2011. Converging evidence for an association of $ATP2B2$ allelic variants with autism in male subjects. *Biol. Psychiatry* 70, 880–887.
- Chen, J., Daggett, H., De Waard, M., Heinemann, S.H., Hoshi, T., 2002. Nitric oxide augments voltage-gated P/Q-type Ca^{2+} channels constituting a putative positive feedback loop. *Free Radic. Biol. Med.* 32, 638–649.
- DeMarco, S.J., Strehler, E.E., 2001. Plasma membrane Ca^{2+} -atpase isoforms 2b and 4b interact promiscuously and selectively with members of the membrane-associated guanylate kinase family of PDZ (PSD95/Dlg/ZO-1) domain-containing proteins. *J. Biol. Chem.* 276, 21594–21600.
- Empson, R.M., Turner, P.R., Nagaraja, R.Y., Beesley, P.W., Knopfel, T., 2010. Reduced expression of the Ca^{2+} transporter protein $PMCA2$ slows Ca^{2+} dynamics in mouse cerebellar Purkinje neurons and alters the precision of motor coordination. *J. Physiol.* 588, 907–922.
- Fernandes, D., Zaidi, A., Bean, J., Hui, D., Michaelis, M.L., 2007. RNA-induced silencing of the plasma membrane Ca^{2+} -ATPase 2 in neuronal cells: effects on Ca^{2+} homeostasis and cell viability. *J. Neurochem.* 102, 454–465.
- Froehner, S.C., 1993. Regulation of ion channel distribution at synapses. *Annu. Rev. Neurosci.* 16, 347–368.
- Gallo, E.F., Iadecola, C., 2011. Neuronal nitric oxide contributes to neuroplasticity-associated protein expression through cGMP, protein kinase G, and extracellular signal-regulated kinase. *J. Neurosci.* 31, 6947–6955.
- Garcia, M.L., Murray, K.D., Garcia, V.B., Strehler, E.E., Isackson, P.J., 1997. Seizure-induced alterations of plasma membrane calcium ATPase isoforms 1, 2 and 3 mRNA and protein in rat hippocampus. *Brain Res. Mol. Brain Res.* 45, 230–238.
- Garside, M.L., Turner, P.R., Austen, B., Strehler, E.E., Beesley, P.W., Empson, R.M., 2009. Molecular interactions of the plasma membrane calcium ATPase 2 at pre- and post-synaptic sites in rat cerebellum. *Neuroscience* 162, 383–395.
- Gotti, S., Sica, M., Vigiletti-Panzica, C., Panzica, G., 2005. Distribution of nitric oxide synthase immunoreactivity in the mouse brain. *Microsc. Res. Tech.* 68, 13–35.
- Gruel, D.L., Franklin, C.L., 1987. Morphological and physiological differentiation of Purkinje neurons in cultures of rat cerebellum. *J. Neurosci.* 7, 1271–1293.
- Hockberger, P.E., Tseng, H.Y., Connor, J.A., 1989. Development of rat cerebellar Purkinje cells: electrophysiological properties following acute isolation and in long-term culture. *J. Neurosci.* 9, 2258–2271.
- Jeromin, A., Haganir, R.L., Linden, D.J., 1996. Suppression of the glutamate receptor delta 2 subunit produces a specific impairment in cerebellar long-term depression. *J. Neurophysiol.* 76, 3578–3583.
- Kitano, J., Nishida, M., Itsukaichi, Y., Minami, I., Ogawa, M., Hirano, T., Mori, Y., Nakanishi, S., 2003. Direct interaction and functional coupling between metabotropic glutamate receptor subtype 1 and voltage-sensitive Ca^{2+} channel. *J. Biol. Chem.* 278, 25101–25108.
- Klemmer, P., Smit, A.B., Li, K.W., 2009. Proteomic analysis of immunoprecipitated synaptic protein complexes. *J. Proteomics* 72, 82–90.
- Kovacs, A.D., Cebers, G., Ceber, A., Liljequist, S., 2002. Selective and AMPA receptor-dependent astrocyte death following prolonged blockade of glutamate reuptake in rat cerebellar cultures. *Exp. Neurol.* 174, 58–71.
- Kozel, P.J., Friedman, R.A., Erway, L.C., Yamoah, E.N., Liu, L.H., Riddle, T., Duffy, J.J., Doetschman, T., Miller, M.L., Cardell, E.L., et al., 1998. Balance and hearing deficits in mice with a null mutation in the gene encoding plasma membrane Ca^{2+} -ATPase isoform 2. *J. Biol. Chem.* 273, 18693–18696.
- Kozel, P.J., Davis, R.R., Krieg, E.F., Shull, G.E., Erway, L.C., 2002. Deficiency in plasma membrane calcium ATPase isoform 2 increases susceptibility to noise-induced hearing loss in mice. *Hear. Res.* 164, 231–239.
- Kurnellas, M.P., Lee, A.K., Li, H., Deng, L., Ehrlich, D.J., Elkabes, S., 2007. Molecular alterations in the cerebellum of the plasma membrane calcium ATPase 2 ($PMCA2$)-null mouse indicate abnormalities in Purkinje neurons. *Mol. Cell. Neurosci.* 34, 178–188.
- Kurnellas, M.P., Li, H., Jain, M.R., Giraud, S.N., Nicot, A.B., Ratnayake, A., Heary, R.F., Elkabes, S., 2010. Reduced expression of plasma membrane calcium ATPase 2 and collapsin response mediator protein 1 promotes death of spinal cord neurons. *Cell Death Differ.* 17, 1501–1510.
- Lee, J.I., O'Halloran, D.M., Eastham-Anderson, J., Juang, B.T., Kaye, J.A., Scott Hamilton, O., Lesch, B., Goga, A., L'Etoile, N.D., 2010. Nuclear entry of a cGMP-dependent kinase converts transient into long-lasting olfactory adaptation. *Proc. Natl. Acad. Sci. U. S. A.* 107, 6016–6021.
- Lev-Ram, V., Wong, S.T., Storm, D.R., Tsien, R.Y., 2002. A new form of cerebellar long-term potentiation is postsynaptic and depends on nitric oxide but not cAMP. *Proc. Natl. Acad. Sci. U. S. A.* 99, 8389–8393.

- Marcoli, M., Maura, G., Cervetto, C., Giacomini, C., Oliveri, D., Candiani, S., Pestarino, M., 2006. Nitric oxide-evoked cGMP production in Purkinje cells in rat cerebellum: an immunocytochemical and pharmacological study. *Neurochem. Int.* 49, 683–690.
- Marcos, D., Sepulveda, M.R., Berrocal, M., Mata, A.M., 2009. Ontogeny of ATP hydrolysis and isoform expression of the plasma membrane Ca²⁺-ATPase in mouse brain. *BMC Neurosci.* 10, 112.
- Namiki, S., Kakizawa, S., Hirose, K., Iino, M., 2005. NO signalling decodes frequency of neuronal activity and generates synapse-specific plasticity in mouse cerebellum. *J. Physiol.* 566, 849–863.
- Nicot, A., Ratnakar, P.V., Ron, Y., Chen, C.C., Elkabes, S., 2003. Regulation of gene expression in experimental autoimmune encephalomyelitis indicates early neuronal dysfunction. *Brain* 126, 398–412.
- Ota, K.T., Monsey, M.S., Wu, M.S., Schafe, G.E., 2010. Synaptic plasticity and NO-cGMP-PKG signaling regulate pre- and postsynaptic alterations at rat lateral amygdala synapses following fear conditioning. *PLoS One* 5, e11236.
- Pottorf II, W.J., Johanns, T.M., Derrington, S.M., Strehler, E.E., Enyedi, A., Thayer, S.A., 2006. Glutamate-induced protease-mediated loss of plasma membrane Ca²⁺ pump activity in rat hippocampal neurons. *J. Neurochem.* 98, 1646–1656.
- Prasad, V., Okunade, G., Liu, L., Paul, R.J., Shull, G.E., 2007. Distinct phenotypes among plasma membrane Ca²⁺-ATPase knockout mice. *Ann. N.Y. Acad. Sci.* 1099, 276–286.
- Sgambato-Faure, V., Xiong, Y., Berke, J.D., Hyman, S.E., Strehler, E.E., 2006. The Homer-1 protein Ania-3 interacts with the plasma membrane calcium pump. *Biochem. Biophys. Res. Commun.* 343, 630–637.
- Shibuki, K., Kimura, S., 1997. Dynamic properties of nitric oxide release from parallel fibers in rat cerebellar slices. *J. Physiol.* 498, 443–452.
- Shigemoto, R., Abe, T., Nomura, S., Nakanishi, S., Hirano, T., 1994. Antibodies inactivating mGluR1 metabotropic glutamate receptor block long-term depression in cultured Purkinje cells. *Neuron* 12, 1245–1255.
- Shin, J.H., Linden, D.J., 2005. An NMDA receptor/nitric oxide cascade is involved in cerebellar LTD but is not localized to the parallel fiber terminal. *J. Neurophysiol.* 94, 4281–4289.
- Souayah, N., Sharovetskaya, A., Kurnellas, M.P., Myerson, M., Deitch, J.S., Elkabes, S., 2008. Reductions in motor unit number estimates (MUNE) precede motor neuron loss in the plasma membrane calcium ATPase 2 (PMCA2)-heterozygous mice. *Exp. Neurol.* 214, 341–346.
- Spiden, S.L., Bortolozzi, M., Di Leva, F., de Angelis, M.H., Fuchs, H., Lim, D., Ortolano, S., Ingham, N.J., Brini, M., Carafoli, E., Mammano, F., Steel, K.F., 2008. The novel mouse mutation Oblivion inactivates the PMCA2 pump and causes progressive hearing loss. *PLoS Genet.* 10, e1000238.
- Stauffer, T.P., Guerini, D., Carafoli, E., 1995. Tissue distribution of the four gene products of the plasma membrane Ca²⁺ pump. A study using specific antibodies. *J. Biol. Chem.* 270, 12184–12190.
- Steinberg, J.P., Takamiya, K., Shen, Y., Xia, J., Rubio, M.E., Yu, S., Jin, W., Thomas, G.M., Linden, D.J., Huganir, R.L., 2006. Targeted *in vivo* mutations of the AMPA receptor subunit GluR2 and its interacting protein PICK1 eliminate cerebellar long-term depression. *Neuron* 49, 845–860.
- Suarez, I., Bodega, G., Rubio, M., Felipe, V., Fernandez, B., 2005. Neuronal and inducible nitric oxide synthase expression in the rat cerebellum from portacaval anastomosis. *Brain Res.* 1047, 205–213.
- Womack, M.D., Khodakhah, K., 2003. Somatic and dendritic small-conductance calcium-activated potassium channels regulate the output of cerebellar Purkinje neurons. *J. Neurosci.* 23, 2600–2607.
- Womack, M.D., Walker, J.W., Khodakhah, K., 2000. Impaired calcium release in cerebellar Purkinje neurons maintained in culture. *J. Gen. Physiol.* 115, 339–346.
- Womack, M.D., Chevez, C., Khodakhah, K., 2004. Calcium-activated potassium channels are selectively coupled to P/Q-type calcium channels in cerebellar Purkinje neurons. *J. Neurosci.* 24, 8818–8822.
- Xu, L., Mabuchi, T., Katano, T., Matsumura, S., Okuda-Ashitaka, E., Sakimura, K., Mishina, M., Ito, S., 2007. Nitric oxide (NO) serves as a retrograde messenger to activate neuronal NO synthase in the spinal cord via NMDA receptors. *Nitric Oxide* 17, 18–24.